HHS Public Access

Author manuscript

Oncogene. Author manuscript; available in PMC 2015 December 23.

Published in final edited form as:

Oncogene. 2015 May 7; 34(19): 2437–2449. doi:10.1038/onc.2014.189.

Inhibition of BMP Signaling Suppresses Metastasis in Mammary Cancer

P. Owens[1], **M. W. Pickup**[1], **S. V. Novitskiy**[1], **J. M. Giltnane**[2], **A. E. Gorska**[1], **C. R. Hopkins**[3], **C. C. Hong**[4,5,♯], and **H. L. Moses**[1,2,♯]

[1]Department of Cancer Biology and Vanderbilt-Ingram Cancer Center

[2]Department of Pathology, Microbiology and Immunology

[3]Departments of Pharmacology and Chemistry, Vanderbilt Center for Neuroscience Drug Discovery

[4]Research Medicine, Veterans Affairs TVHS, Nashville, TN 37212

[5]Division of Cardiovascular Medicine, Vanderbilt University School of Medicine, Nashville, TN 37232

Abstract

Bone Morphogenetic Proteins (BMPs) are secreted cytokines/growth factors that play differing roles in cancer. BMPs are overexpressed in human breast cancers, but loss of BMP signaling in mammary carcinomas can accelerate metastasis. We show that human breast cancers display active BMP signaling, which is rarely downregulated or homozygously deleted. We hypothesized that systemic inhibition of BMP signaling in both the tumor and the surrounding microenvironment could prevent tumor progression and metastasis. To test this hypothesis, we used DMH1, a BMP antagonist, in MMTV.PyVmT expressing mice. Treatment with DMH1 reduced lung metastasis and the tumors were less proliferative and more apoptotic. In the surrounding tumor microenvironment, treatment with DMH1 altered fibroblasts, lymphatic vessels and macrophages to be less tumor promoting. These results indicate that inhibition of BMP signaling may successfully target both the tumor and the surrounding microenvironment to reduce tumor burden and metastasis.

Keywords

BMP; DMH1; Metastasis; Tumor Microenvironment; Breast Cancer

Corresponding Author: Philip Owens, Vanderbilt University, philip.owens@vanderbilt.edu, Phone: 1-(615) 936-1511, Fax: 1-(615) 936-5859.

♯Senior co-authors, Vanderbilt University, Nashville TN 37232.

Conflict of interest

The authors have no conflicts of interest to declare.

Introduction

Bone morphogenetic proteins (BMPs) are secreted cytokine/growth factors belonging to the Transforming Growth Factor β superfamily known for their pleiotropic functions. BMPs have been historically defined by osteo-inductive capabilities, as well as roles in early embryologic cell fate specification(1, 2). The BMP pathway consists of a well-defined signaling cascade that begins with translation of more than 20 ligands, which must be processed and bound to receptors as either homo or heterodimers(1). In the extracellular space, ligands can be regulated by many secreted soluble antagonists including Noggin, Chordin and Gremlin(1). Ligand binding stimulates type I and type II receptor serine/threonine kinase phosphorylation, which in turn phosphorylate intracellular Smad proteins [Smads 1, 5 and 8(mouse)/9(human)]. Phosphorylated Smads then partner with Smad4 to translocate to the nucleus, where they regulate the transcription of target genes, particularly *Id1* as the canonical BMP response gene(1). BMPs also induce *Smad6*, which functions to block receptor Smad phosphorylation and promote receptor turnover, providing a finely tuned negative feedback signaling pathway(3).

New roles for BMPs in cancer have been identified. The function of BMP mutation was described in Juvenile Polyposis Syndrome (JPS-OMIM#174900) patients, where BMPR1A is mutated and leads to benign hamartomas(4, 5). Loss of function mouse experiments in skin also demonstrated benign hamartoma tumor formation when BMPR1a was absent or lost(6–9). It has recently been shown that the BMP antagonist DAND5 (also known as COCO) can regulate the reactivation of dormant metastatic breast cancer cells in the lung(10). Additional tumor suppressive roles of BMP signaling have been identified in our previous studies overexpressing a dominant negative form of the type II BMP receptor (BMPR2)(11). However, BMPs have also shown a dual role in cancer, similar to TGFβ(12, 13). Much like TGFβ, BMP stimulation of tumor cells has demonstrated growth inhibition, while enhancing cell migration and invasion (14, 15). BMPs have also been shown to antagonize the TGFβ directed epithelial to mesenchymal transition (EMT)-stem cell-like phenotype(16, 17). This may suggest a role for BMPs in reversing the tumor promoting EMT process, thereby promoting a mesenchymal to epithelial transition, such as the reactivation of dormant cancer stem cells via COCO(10).

Unlike the dual roles of BMP function in the tumor, BMP-stimulated cells in the surrounding tumor microenvironment typically have a tumor promoting phenotype based on *in vitro* studies. BMP stimulation of fibroblasts can promote prostate tumor angiogenesis(18). We found that BMP stimulation of mammary fibroblasts resulted in enhanced tumor cell invasion and increased inflammatory cytokine secretion and matrix remodeling factors(19). BMPs can also stimulate lymphangiogenesis, which may be utilized by tumors to facilitate metastatic dissemination(20). When macrophages are stimulated by BMP ligands, they produce inflammatory cytokines that could promote tumor progression and metastasis(21–24).

The use of small molecule BMP antagonists has recently been shown to successfully reduce prostate to bone metastases, lung cancer cell growth and reduce primary tumor growth of mammary carcinomas(25–27). BMP inhibition in breast cancer reduces tumor growth by

inhibiting the cancer stem cell self-renewal via the p63 signaling network(25). DMH1, a second-generation analog of dorsomorphin (DM), is a highly selective small molecule inhibitor of BMP receptor (28–30). In contrast to DM and the first-generation analog LDN-193189, both of which target TGFβ type-2 receptor, AMP-activated kinase, VEGF type-2 receptor, DMH1 does not inhibit these kinases (30). Moreover, in contrast to other reported BMP inhibitors (31), DMH1 does not significantly inhibit the TGFβ type-I receptors, ALK4 and ALK5 (30). Thus, DMH1 is the most selective of the published small molecule inhibitors of BMP signaling, with IC50 (concentration causing 50% of inhibition) of 27, 108, <5 and 48 nM against the type-1 receptors ALK1, ALK2, ALK3 and ALK6, respectively.

We hypothesize that BMP signaling is largely intact in breast cancer and dynamically active in the tumor microenvironment, which may provide a unique therapeutic target of an understudied pathway. We show in a murine breast cancer model that systemic inhibition of BMP activity in both the tumor and the surrounding microenvironment reduces pulmonary metastases.

Results

Human breast cancers and their metastases retain active BMP signaling

BMP ligands are overexpressed in human breast cancers(32–35). We sought to determine whether the BMP signaling pathway is active or absent in breast tumor cells as well as in the tumor microenvironment. Immunohistochemistry (IHC) for pSmad1/5/9 demonstrated strong reactivity in the epithelium as well as the surrounding stroma in normal human breast, hyperplasia, Ductal Carcinoma In Situ (DCIS), Invasive Ductal Carcinomas (IDC) and metastases to brain, bone, liver and lung (Fig. 1a–h). Quantified scoring of two human breast tissue microarrays containing samples that were subdivided into normal, ADH-CIS (atypical ductal hyperplasia-carcinoma in situ) and invasive revealed active BMP signaling (Fig. 1i). In order to determine whether TGFβ/BMP/Activin receptors correlate with the survival of breast cancer patients we turned to the publicly available database kmplotter (kmplot.com). We compared expression of TGFβ and Activin receptors correlating with relapse free survival (RFS) in breast cancer and found that high levels of either the type I or type II receptors correlate with improved RFS (Fig. S1a–h). Interestingly, we found that the two common core receptors that mediate BMP signaling (*BMPR1A* and *BMPR2*) displayed the opposite trend and demonstrated that high *BMPR1A* and *BMPR2* receptor expression correlates with poor RFS (fig. 1J &1k).

Breast cancers do not frequently lose BMP signaling components

The recent publication of TCGA (The Cancer Genome Atlas) for breast cancer has made it possible to determine significance of gene expression changes(36). We utilized the cBio portal to search the TCGA database for changes in BMP signaling components(37, 38). We discovered that 21 genes involved in BMP signaling were altered in at least 5% of the 950 patient samples in the provisional breast TCGA database (Fig. 1l). Of the 21 genes, we found that only *SMAD4* and *BMP1* were reduced in human breast cancer. It should be noted that while Smad4 mediates canonical BMP signaling, it also functions as a tumor suppressor

via TGFβ and Activin(39). Most BMP signaling components were not absent or decreased, but actually amplified and/or upregulated, including ligands *BMP2, BMP5, BMP6* and *BMP7* (Fig. 1l) which has previously been reported independently of the TCGA(32, 35). What may confuse matters is that not only are ligands being upregulated, but also their secreted antagonists such as *NOGGIN, CHORDIN* and *GREMLIN* appeared upregulated as well (Fig. 1l). BMP receptor homozygous deletion and downregulation in TCGA patients were extremely rare, and were countered with more patients that displayed upregulation of BMP receptors (Fig. 1l & Supplementary Table S1). We searched for these 21 BMP-related genes in 59 breast cancer cell lines and found higher percentages of alterations were represented for these BMP signaling components (Fig. S1i). The largest difference was for *BMP7*, which was only altered in 12% of human patient samples (Fig. 1l) and altered in 46% of cell lines (Fig. S1e), of which almost all changes were upregulation or gene amplification.

Administration of DMH1 to mice reduces tumor burden

Recent studies have demonstrated that inhibition of BMP signaling in breast and prostate cancer can potentially provide therapeutic benefit(25, 27). Mice expressing the oncogene Polyoma Middle T (PyVmT) have active pSmad1/5/8 in their primary tumors and metastases(11). Female mice expressing MMTV.PyVmT were examined beginning at three weeks of age, and upon tumor palpation were implanted with a 6 week slow-release osmotic pump containing vehicle (DMSO) or DMH1 (Fig. 2a). After six weeks of treatment, tumors were removed and H&E stained, which revealed that vehicle treated tumors exhibited advanced carcinoma histology (Fig. 2b–c). Examination of H&E sections of the liver and kidneys showed no evidence of toxicity associated with DMH1 administration (Fig. S2). While the primary tumor size was not significantly altered (Fig. S3a–b), the number of primary tumors was significantly ($P=0.014$) reduced in DMH1 treated animals (Fig. 2d). We next stained primary tumors for the proliferation marker Ki-67 and found that treatment of tumors with DMH1 significantly ($P=0.001$) reduced the number of Ki-67 positive tumor cells (Fig. 2e–g). We then examined for apoptosis by IHC for cleaved caspase-3 and found a significant ($P=0.016$) increase in positive cells in DMH1 treated primary tumors (Fig. 2h–j). This discrepancy between tumor size, tumor number and proliferation from Ki-67 IHC may be partially explained in the nature of the spontaneous tumors ability to have different changes in stroma, tumor cells and cystic fluid filled tumors. To determine whether BMPR1a (the target of DMH1) was inhibited, we performed pSmad1/5/8 IHC, which revealed strong active BMP staining in vehicle (Fig. 2k) treated tumors, and diminished staining in DMH1 treated tumors (Fig. 2l). To further validate whether tumors had a specific response to BMP inhibition, we performed FACS isolation of epithelial cells and measured three genes known to be active targets of BMP transcription(1). Both *Smad6* and *Id1* transcription were significantly downregulated with DMH1 treatment (Fig. 2m). *Smad7* is also a transcriptional target of BMP signaling, but may also be indicative of TGFβ family signaling and not always specific to BMP signaling inhibited by DMH1. Because another BMP inhibitor (LDN-193189) was recently shown to reduce primary tumor growth and demonstrated a reduction in basal or cancer stem cells, we investigated changes in cell lineages in the tumors(25). We found that ΔNp63 was not significantly altered in IHC (Fig. S3c–d) or by qPCR (Fig. S3e), yet other basal factors such as *K14* were altered, and

inversely correlated with *K18* expression (Fig. S3e). Further qPCR analysis demonstrated that DMH1 tumor cells did in fact show a reduction in key EMT/Stem cell-like related genes such as *Snail*, *Twist*, *Zeb1* and *Zeb2* (Fig S3f). And while qPCR had a trend towards less *Vimentin* and increased *Ecadherin* (Fig. S3f), no appreciable differences were observed by IF staining for luminal (K8/18) and basal (K5) markers as well as EMT indicators Ecadherin and Vimentin (Fig. S3g–j).

DMH1 treatment inhibits pulmonary metastases

While a recent report had demonstrated reduction in mouse mammary tumors treated with a BMP inhibitor(25), we were curious to investigate the impact on metastasis. The MMTV-PyVmT model is widely used because of its full metastatic penetrance phenotype, with animals consistently developing pulmonary metastases (40). When 12 mice were compared for both treatments it was found that a significant reduction in metastases occurred in DMH1 treated mice (Fig. 3a–c). Once lung metastases were counted, they were sectioned and stained again with H&E, which confirmed the presence of PyVmT-carcinoma derived metastases (Fig. 3d–e). To verify that DMH1 treatment had reduced BMP signaling, we performed IHC and found a reduction in pSmad1/5/8 staining with DMH1 treatment (Fig. 3f–g). At the time of sacrifice, 0.5ml of peripheral blood was removed by cardiac puncture and RNA was isolated to detect the presence of circulating tumor cells. qPCR for BMP response gene *Id1* was found to be significantly lower, as were other markers of tumor epithelia and the oncogene transgene itself in DMH1 treated animals (Fig. 3h).

DMH1 treatment reduces the fibrotic response in tumors

We have recently published work demonstrating how BMP stimulation of mammary fibroblasts *in vitro* can promote mammary carcinoma invasion(19). We hypothesized that, similar to *in vitro* experiments, DMH1 could reduce the tumor enhancing effects of cancer-associated fibroblasts. Upon examination of the tumor stroma, we noticed that vehicle treated tumors appeared largely filled with carcinoma cells and that collagen (highlighted by aniline blue) staining in Masson trichrome was abundant within the tumor (Fig. 4a). Tumors treated with DMH1 had large regions of stroma with limited amounts of collagen (Fig. 4b). We further investigated the tumor-stroma interface by performing IF staining for Collagen I, which highlights the basement membrane around the tumors. Vehicle treated tumors displayed a different staining pattern from that found with DMH1 treated tumors (Fig. 4c–d). We next performed IF staining Collagen IV and found the nature of fibers to follow the pattern indicated by trichrome and Collagen I IF staining (Fig. S4a–b). To further investigate collagen fibers, we stained tumors with Picrosirius red, which when viewed under polarized light can indicate the density of fibers. We did not find any morphological differences or significance in the intensity of birefringence from collagen fibers stained with Picrosirius red (Fig. S4c–g). IF staining for Fibronectin was sparsely populated in both the vehicle and DMH1 treated tumors (Fig. S4h–i). Cancer associated fibroblasts can be identified by the myofibroblast marker αSMA for which we performed IF staining and found a significant ($P=0.03$) reduction in DMH1 treated primary tumors (Fig. 4e–g). αSMA also marks blood vessels and myoepithelial cells in addition to cancer associated fibroblasts. To probe deeper into the nature of the tumor-associated fibroblasts, we used the marker PDGFRα+ to identify fibroblasts in primary tumors (Fig. 4h). We found that DMH1 treated tumors had a

slight, but not significant, increase in fibroblasts in primary tumors compared with vehicle treated animals (Fig. 4i–k). To determine how these fibroblasts were functionally different when treated with DMH1, we isolated PDGFRα+ cells using FACS and performed qPCR. We found that the DMH1 treated fibroblasts gene expression was less tumor promoting with increased *Cav1* and decreased *Adam17*. Crosslinking factors known to promote metastasis and matrix stiffness *Lox* and *Loxl2*(41–44) were also significantly reduced with DMH1 treatment (Fig. 4l). qPCR also demonstrated a reduction in αSMA in fibroblasts from DMH1 treated tumors (Fig. 4l). In agreement with our previous findings in vitro(19), DMH1 treatment of primary tumors reduced *Mmp2* and *Ccl9* in fibroblasts (Fig. 4l). Both of these factors are known to promote invasion and metastases, and can be stimulated by BMP in mouse mammary fibroblasts(19). qPCR also revealed that BMP transcriptional targets *Id1*, *Smad6* and *Smad7* were downregulated in fibroblasts (Fig. S4j).

DMH1 treatment results in decreased lymphatic vessel formation

The BMP pathway has been implicated in lymphatic vessel growth independent of blood vessel growth, and it was suggested that inhibition of BMP signaling during tumor metastatic dissemination could limit lymphatic growth into tumors and subsequently impair metastasis(20). We performed IF for a marker of blood vessels (CD31) and lymphatic vessels (LYVE) in primary tumors and found that vehicle treated tumors contained lymphatic vessels within the tumors (Fig. 5a). DMH1 treated tumors displayed much less LYVE positive cells, and were not located intra-tumorally (Fig. 5b). To observe total vessels, we performed IF staining for the pan-endothelial marker MECA32 and the basement membrane component Laminin. Similar to the architecture seen by H&E staining (Fig. 2b–c) and in Collagen IV IF staining (Fig. S4 a–b), we found that vessel architecture was localized throughout the tumor in vehicle treated animals in contrast to DMH1 treated tumors where vessels remained at the periphery (Fig. 5 c–d). We further investigated the total change in endothelial cells by performing flow cytometry for CD31 and CD102 dual positive cells and found no significant change in blood vessels (Fig. S5a–d). FLT4 (also known as VEGFR3) is a specific receptor on lymphatic cells(45, 46). We found that DMH1 treated tumors contained significantly less VEGFR3+ cells than vehicle control animals (Fig. 5e–h). We additionally performed flow cytometry to analyze the lymphatic specific marker LYVE, and found it was reduced as well in DMH1 treated tumors compared to vehicle controls (Fig. 5i–l). To determine functional differences in lymphatic endothelial cells, we performed FACS of both FLT4+ and LYVE+ cells from primary tumors, isolated RNA and performed qPCR. We found that in both FLT4+ and LYVE-1 positive cells, *Vegfc* expression was significantly down regulated, while the blood vessel growth factor *Vegfa* was not (Fig. 5m). We further investigated the BMP response by qPCR for the FLT4+ and LYVE+ cells and found that BMP response genes *Id1* and *Smad6* were significantly downregulated (Fig. S5e). Taken together, these findings indicate the BMP inhibition with DMH1 can inhibit lymphatic infiltration into tumors.

DMH1 treatment alters myeloid and lymphoid infiltrates to reduce immune promotion of tumors

We first investigated the systemic *in vivo* effect of immune cells with DMH1 inhibition, and found that the total number of myeloid and immune cells (CD45+) were significantly higher

in DMH1 treated animals compared to vehicle controls (Fig. 6a–d). T cell specific staining demonstrated modest changes for CD8+ T cells (increased in DMH1 treated tumors); however, CD3+ and CD4+ cells were not affected (Fig. S6a–d). We proceeded to investigate if myeloid cell lineages were altered, and found that Gr-1+ cells were not different in their percentage in the primary tumors (Fig. S6e–h). Interestingly, qPCR analysis of FACS isolated Gr1+ cells found that DMH1 treated tumors were found to have less *iNos* and *Arg*inase gene expression (Fig. S6i). We next examined macrophages by flow cytometry and found that there were more F4/80+ macrophages in primary tumors treated with DMH1 than vehicle controls (Fig. 6e–h). We next localized these macrophages with IF staining and found that F4/80 macrophages were localized within the tumor, while DMH1 treatment resulted in macrophages being localized at the periphery of the tumors (Fig. 6-i-j). IF staining for CD206 (mannose receptor), which has been indicative of the putative "M2 polarization" for tumor promoting macrophages(47) were densely found throughout the vehicle treated tumors, yet reduced in DMH1 treated primary tumors (Fig. 6k–l). Additionally, several genes known to promote metastasis and tumor progression from macrophages, were found to be significantly reduced such as *iNos*, *Cox2*, *Ccl5*, *Il18* and *Il10* (Fig. 6m). These results indicate that myeloid cells are responsive to BMP inhibition and this results in a less tumor promoting phenotype.

We next sought to test the direct effect of DMH1 on monocytes. We isolated hematopoietic stem cells from femur flushes of C67BL6 females and converted the cells to monocytes by treatment with M-CSF for 7 days (Fig. 7a). These monocyte cells were either left in normal medium, treated with recombinant mouse BMP4, or recombinant BMP4 and DMH1. We isolated RNA and synthesized cDNA and performed qPCR from these cells and found that almost universally BMP4 stimulation had no effect on gene expression. However with DMH1 treatment monocytes had significant reduction in expression of *Arg1*, *Il10* and *Il4* which are genes known for promoting immunosuppression in tumors as well as alternate M2 polarization of monocytes (Fig. 7b). We next examined gene expression for *Mmp2*, *Mmp9* and *Mmp13* and found that these genes where significantly decreased with DMH1 treatment. Finally, we performed qPCR for genes indicating specific attenuation of the BMP pathway with target genes *Id1*, *Smad6* and *Smad7*, which were all significantly decreased with DMH1 inhibition (Fig. 7d). Interestingly, BMP4 stimulation was either unresponsive or what may be a saturation of BMP activity in monocyte cells that could only be reduced and not enhanced (Fig. 7b–d)

Discussion

BMP signaling has largely been regarded to be tumor suppressive based on the landmark studies by Howe et al. demonstrating the loss of BMPR1a in the formation of Juvenile Polyposis Syndrome(4). Interestingly, the loss of BMPR1a results in hamartomas, which are typically benign tumors(48). Recently, analysis from the TCGA revealed that while TGFβ and Activin signaling components are frequently mutated, BMPR1a and other BMP specific signaling components are not(49). These results suggest that many tumors may require core developmental signaling pathways such as BMP signaling in order to progress and even metastasize. Similar to TGFβ, it is a common mistake to simply label a pathway as tumor suppressive or promoting. Like TGFβ, BMPs are being found to have distinct functions that

can both support and restrict tumorignesis(13). Further studies that define BMP activity within the cells context and function will enhance decisions for patient therapy.

The BMP pathway has recently been considered for therapeutic intervention. In prostate cancer, a recent report has shown that use of the Dorsomorphin analog LDN-193189 can be used to block bone metastases by inhibiting the tumor cells mimicry of the bone microenvironment(27). This is a rational strategy, originating from the hypothesis of the so called “vicious-cycle” whereby tumor cells participate in the turnover of the bone, potentially hijacking BMPs ability for osteoinduction that could be co-opted with the tumor’s cells(49). BMP signaling has been shown to enhance human breast cancer cells metastasis to the bone(50). BMP inhibition with LDN-193189 has now been used in mouse models of breast cancer and shown to inhibit the ability of these tumors to self-renew via ΔNp63(25). Interestingly, LDN-193189 is known to inhibit more than just BMPR kinase activity, and could potentially represent a therapeutic option that inhibits VEGFR and other known off-targets(51).

In this study, we show that BMP signaling remains high in both carcinoma and stromal cells in human breast cancer, that high expression of BMP receptors is associated with less relapse free survival, and that genes encoding proteins involved in BMP signaling are rarely deleted or mutated in human breast cancers. Gene amplification and/or overexpression are relatively frequent. To test the significance of BMP signaling, we used the small molecule BMP antagonist, DMH1, in a mouse model of breast cancer and demonstrate that it suppresses pulmonary metastases. We show that systemic inhibition of the BMP pathway (which is active in both the tumor cells and the surrounding tumor microenvironment) demonstrates anti-metastatic function. Changes in stromal volume were not affected by DMH1 with regard to the percentage of cells that are fibroblasts (Fig. 4k), only partially in lymphatics (Fig. 5h&l), and significantly for immune cells (Fig. 6d&h). The ratio of stroma to tumor is a dynamic process in cancer and further studies will potentially uncover how therapeutics successfully affects the ratio of these distinct cell populations. Our rationale has been supported by *in vitro* reports of BMP tumor promoting effects in tumor cells(14, 15, 27, 34, 52–54), fibroblasts(18, 19), lymphatics(20) and immune components(21–24, 55) of the tumor microenvironment. While many anti-cancer strategies target a single or unique cell population, we demonstrate an approach that can integrate multiple cell types for therapeutic targeting of mammary carcinoma metastasis.

Methods

Mice, Treatments and surgical pump implantation

All animal experiments were performed at Vanderbilt University and approved by IACUC. FVBn mice were purchased from Harlan and were used to maintain the MMTV.PyVmT transgene, which were PCR genotyped as previously described(11). Mice were weaned at three weeks of age and female mice were genotyped for the PyVmT transgene, and were then palpated for tumors twice weekly. Animals that had a palpable tumor were implanted the following day with either DMSO (Sigma) or DMH1 containing osmotic pump (Alzet). Six-week pumps containing 200ul of either DMSO or 35mg/ml of DMH1 were surgically placed into the right flank of mice. Mice were monitored daily for health and welfare and

following six weeks were euthanized in accordance with IACUC. Immediately following euthanasia, 0.5ml blood was isolated and placed into RNAlater (Ambion). Collection of tumor tissue was performed by dissecting the tumor to be snap-frozen tissue in LN^2, OCT and formalin fixed paraffin embedding. Lungs were inflated with 2–3ml of heparin (50ug/ml), fixed in 10% neutral buffered formalin and dehydrated, cleared in xylene, rehydrated, stained with Mayer's hematoxylin, dehydrated and metastatic lung foci quantitated. Lungs were then embedded in paraffin and sectioned for histology.

Immunohistochemistry and Immunofluorescence

Human tissues from were acquired through de-identified tissues from the Cooperative Human Tissue Network at Vanderbilt University. Tissue microarray were purchased from US. BioMax (cat# BR480 and BR722). Tissues paraffin embedded were sectioned at 5uM and dewaxed in xylene and rehydrated in alcohol with citrate antigen retrieval as previously described(11). Standard Mayers hematoxylin and eosin (H&E) was performed. Picrosirus red staining was performed as previously described and visualized with and without polarized light(56). Masson's Trichrome (Sigma) was stained as described previously (11). The following antibodies were used at the specified primary dilutions: pSmad1/5/8 (Cell Signaling Cat#9511, 1:200), Ki-67 (Novocastra #MM1, 1:200), Cleaved Caspase-3 (Cell Signaling Cat#9661, 1:200), DNp63 (Santa Cruz Cat#H129 1:200), Collagen IV (Abcam Cat#ab6586 1:500), K8/18 (RDI-Fitzgerald Cat#20R-CP004 1:500), CD31 (BD Cat# 1:200), LYVE (RDI-Fitzgerald Cat#70R-LR003 1:100), MECA32 (BD Cat#550563 1:200), Laminin (RDI-Fitzgerald # 1:200), F4/80 (Invitrogen #MF48000 1:50), CD206 (BioLegend Cat#141701 1:100) K5 (Covance Cat#PRB-160P-100 1:500), Ecadherin (BD Cat#610182 1:200), Vimentin (Covance Cat#PCK-594P 1:500), aSMA (Sigma Cat#A2547 1:500). Paraffin derived sections were counterstained with hematoxylin (Vector Labs QS) and mounted with Cytoseal. Frozen sections were cut at 8uM and fixed in 4%PFA containing . 1% Triton-X for 20 minutes. Immunofluorescence staining was performed with primary and secondary antibodies diluted in 12% Fraction V BSA (Pierce) and slides were mounted in SlowFade mounting medium containing DAPI (Invitrogen). All fluorescent secondary antibodies were highly cross-adsorbed produced in goat and used at a dilution of 1:200 for 20 minutes (Molecular Probes). Quantification of IHC and IF was performed using NIH ImageJ (http://rsbweb.nih.gov/ij/docs/examples/stained-sections/index.html) and as previously described(57).

Flow Cytometry and single sorting (FACS)

Single-cell suspensions were made from primary tumors as previously described(58, 59). Cells were stained with fluorescence-conjugated antibodies (BioLegend, eBioscience, BD) and isotype matched IgG controls. The cells were analyzed on a LSRII flow cytometer (BD). FACS was performed with a FACSAria flow cytometer (BD) EpCAM+CD45-PDGFRa-, PDGFRa+CD45-EpCAM-, FLT4+CD45-EpCAM-PDFRa-, LYVE+ CD45-EpCAM-PDFRa-, CD45+EpCAM-CD11b+F4/80+, CD45+Gr1+ cell were collected for gene expression analysis. DAPI was used to exclude dead cells.

RNA Isolation, cDNA synthesis, qPCR and fibroblast cell culture-scratch assay

RNA isolation of snap-frozen tissue was performed by placing tissue directly into Trizol (Invitrogen) and purified by chloroform and alcohol precipitation. Trizol isolated RNA was then subjected to cleanup with RNeasy purification including DNAseI treatment as was cells isolated from FACS. RNA from blood was purified using the Mouse RiboPure Blood RNA Isolation Kit (Ambion) following manufacturer's instructions. Equal amounts of RNA were synthesized into cDNA using the VILO cDNA synthesis kit (Invitrogen). LuminoCt (Sigma) 2X SYBR mastermix was combined with 1uM of both a forward and reverse primer sequence (full table of sequences is listed in Supplemental Table 2) into 20ul reactions and cycled for 95degrees-10s to 60degrees for 30s for 40 cycles followed by a melting curve. BioRad CFX96 was used and instrument provided software was used to determine relative normalized expression to GAPDH expression. Use of human CAF cells were used as previously described(19). Fibroblasts from de-identified breast cancer tissue were cultured at sub-confluence and treated with either vehicle (DMSO) or DMH1(20μM) for 24 hours, following fresh media replacement which was allowed to be conditioned for 48 hours and used to treat a confluent monolayer of HCC1937 human breast cancer cells were 'scratched' to measure tumor migration as described previously(11).

Database utilization and statistical analysis

For analysis of the TCGA dataset, we used the cBio portal (http://www.cbio.portal.org/)(37, 38). Human gene symbols were queried in the provisional dataset and accessed on Jun 3rd 2013. RNA expression cutoff was maintained at the default of 2.0. Analysis of gene expression correlating with RFS was performed using the kmplotter (http://kmplot.com). Human gene symbols were entered into breast and JetSet probe selection was used to determine optimal representative microarray probe(60). Automatic cutoff scores were selected during queries and 10 year RFS were selected. Statistical analysis was performed using Excel (Microsoft), Prism (Graphpad), and FlowJo (TreeStar) software. Statistical significance was deemed for any comparison where $P<0.05$.

Supplementary Material

Refer to Web version on PubMed Central for supplementary material.

Acknowledgements

We would like to thank the members of the Moses laboratory for critically reading the manuscript. We would like to thank Dr. Connor Lynch for help with tissue acquisition. P.O. has been supported by DoD BCRP postdoctoral fellowship grant number W81XWH-09-1-0421. CCH is supported by NIH/NHLBI grants RO1HL104040 and VA Merit Award # 101BX000771. This work is supported by NIH grants CA085492, CA102162, the Robert J. and Helen C. Kleberg Foundation and the T.J. Martell Foundation to HLM. Grant number CA068485 provided core laboratory support.

References

1. Miyazono K, Kamiya Y, Morikawa M. Bone morphogenetic protein receptors and signal transduction. J Biochem. 2010; 147(1):35–51. Epub 2009/09/19. [PubMed: 19762341]
2. Chen D, Zhao M, Mundy GR. Bone morphogenetic proteins. Growth Factors. 2004; 22(4):233–241. Epub 2004/12/29. [PubMed: 15621726]

3. Goto K, Kamiya Y, Imamura T, Miyazono K, Miyazawa K. Selective inhibitory effects of Smad6 on bone morphogenetic protein type I receptors. J Biol Chem. 2007; 282(28):20603–20611. Epub 2007/05/12. [PubMed: 17493940]

4. Howe JR, Bair JL, Sayed MG, Anderson ME, Mitros FA, Petersen GM, et al. Germline mutations of the gene encoding bone morphogenetic protein receptor 1A in juvenile polyposis. Nat Genet. 2001; 28(2):184–187. Epub 2001/05/31. [PubMed: 11381269]

5. Calva-Cerqueira D, Dahdaleh FS, Woodfield G, Chinnathambi S, Nagy PL, Larsen-Haidle J, et al. Discovery of the BMPR1A promoter and germline mutations that cause juvenile polyposis. Hum Mol Genet. 2010; 19(23):4654–4662. Epub 2010/09/17. [PubMed: 20843829]

6. Ming Kwan K, Li AG, Wang XJ, Wurst W, Behringer RR. Essential roles of BMPR-IA signaling in differentiation and growth of hair follicles and in skin tumorigenesis. Genesis. 2004; 39(1):10–25. Epub 2004/05/05. [PubMed: 15124223]

7. Andl T, Ahn K, Kairo A, Chu EY, Wine-Lee L, Reddy ST, et al. Epithelial Bmpr1a regulates differentiation and proliferation in postnatal hair follicles and is essential for tooth development. Development. 2004; 131(10):2257–2268. Epub 2004/04/23. [PubMed: 15102710]

8. Kobielak K, Pasolli HA, Alonso L, Polak L, Fuchs E. Defining BMP functions in the hair follicle by conditional ablation of BMP receptor IA. J Cell Biol. 2003; 163(3):609–623. Epub 2003/11/12. [PubMed: 14610062]

9. Yuhki M, Yamada M, Kawano M, Iwasato T, Itohara S, Yoshida H, et al. BMPR1A signaling is necessary for hair follicle cycling and hair shaft differentiation in mice. Development. 2004; 131(8): 1825–1833. Epub 2004/04/16. [PubMed: 15084466]

10. Gao H, Chakraborty G, Lee-Lim AP, Mo Q, Decker M, Vonica A, et al. The BMP inhibitor Coco reactivates breast cancer cells at lung metastatic sites. Cell. 2012; 150(4):764–779. Epub 2012/08/21. [PubMed: 22901808]

11. Owens P, Pickup MW, Novitskiy SV, Chytil A, Gorska AE, Aakre ME, et al. Disruption of bone morphogenetic protein receptor 2 (BMPR2) in mammary tumors promotes metastases through cell autonomous and paracrine mediators. Proc Natl Acad Sci U S A. 2012; 109(8):2814–2819. Epub 2011/05/18. [PubMed: 21576484]

12. Alarmo EL, Kallioniemi A. Bone morphogenetic proteins in breast cancer: dual role in tumourigenesis? Endocr Relat Cancer. 2010; 17(2):R123–R139. Epub 2010/03/26. [PubMed: 20335308]

13. Ehata S, Yokoyama Y, Takahashi K, Miyazono K. Bi-directional roles of bone morphogenetic proteins in cancer: Another molecular Jekyll and Hyde? Pathol Int. 2013; 63(6):287–296. Epub 2013/06/21. [PubMed: 23782330]

14. Ketolainen JM, Alarmo EL, Tuominen VJ, Kallioniemi A. Parallel inhibition of cell growth and induction of cell migration and invasion in breast cancer cells by bone morphogenetic protein 4. Breast Cancer Res Treat. 2010; 124(2):377–386. Epub 2010/02/26. [PubMed: 20182795]

15. Alarmo EL, Parssinen J, Ketolainen JM, Savinainen K, Karhu R, Kallioniemi A. BMP7 influences proliferation, migration, and invasion of breast cancer cells. Cancer Lett. 2009; 275(1):35–43. Epub 2008/11/05. [PubMed: 18980801]

16. Scheel C, Eaton EN, Li SH, Chaffer CL, Reinhardt F, Kah KJ, et al. Paracrine and autocrine signals induce and maintain mesenchymal and stem cell states in the breast. Cell. 2011; 145(6): 926–940. Epub 2011/06/15. [PubMed: 21663795]

17. Buijs JT, Henriquez NV, van Overveld PG, van der Horst G, Que I, Schwaninger R, et al. Bone morphogenetic protein 7 in the development and treatment of bone metastases from breast cancer. Cancer Res. 2007; 67(18):8742–8751. Epub 2007/09/19. [PubMed: 17875715]

18. Yang S, Pham LK, Liao CP, Frenkel B, Reddi AH, Roy-Burman P. A novel bone morphogenetic protein signaling in heterotypic cell interactions in prostate cancer. Cancer Res. 2008; 68(1):198–205. Epub 2008/01/04. [PubMed: 18172312]

19. Owens P, Polikowsky H, Pickup MW, Gorska AE, Jovanovic B, Shaw AK, et al. Bone Morphogenetic Proteins stimulate mammary fibroblasts to promote mammary carcinoma cell invasion. PloS one. 2013; 8(6):e67533. Epub 2013/07/11. [PubMed: 23840733]

20. Wiley DM, Kim JD, Hao J, Hong CC, Bautch VL, Jin SW. Distinct signalling pathways regulate sprouting angiogenesis from the dorsal aorta and the axial vein. Nat Cell Biol. 2011; 13(6):686–692. Epub 2011/05/17. [PubMed: 21572418]
21. Lee JH, Lee GT, Woo SH, Ha YS, Kwon SJ, Kim WJ, et al. BMP-6 in Renal Cell Carcinoma Promotes Tumor Proliferation through IL-10-Dependent M2 Polarization of Tumor-Associated Macrophages. Cancer Res. 2013; 73(12):3604–3614. Epub 2013/05/02. [PubMed: 23633487]
22. Lee GT, Jung YS, Lee JH, Kim WJ, Kim IY. Bone morphogenetic protein 6-induced interleukin-1beta expression in macrophages requires PU.1/Smad1 interaction. Mol Immunol. 2011; 48(12–13):1540–1547. Epub 2011/05/17. [PubMed: 21571370]
23. Lee GT, Kwon SJ, Lee JH, Jeon SS, Jang KT, Choi HY, et al. Induction of interleukin-6 expression by bone morphogenetic protein-6 in macrophages requires both SMAD and p38 signaling pathways. J Biol Chem. 2010; 285(50):39401–39408. Epub 2010/10/05. [PubMed: 20889504]
24. Hong JH, Lee GT, Lee JH, Kwon SJ, Park SH, Kim SJ, et al. Effect of bone morphogenetic protein-6 on macrophages. Immunology. 2009; 128(1 Suppl):e442–e450. Epub 2009/02/05. [PubMed: 19191909]
25. Balboni AL, Hutchinson JA, DeCastro AJ, Cherukuri P, Liby K, Sporn MB, et al. DeltaNp63alpha-mediated activation of bone morphogenetic protein signaling governs stem cell activity and plasticity in normal and malignant mammary epithelial cells. Cancer Res. 2013; 73(2): 1020–1030. Epub 2012/12/18. [PubMed: 23243027]
26. Langenfeld E, Hong CC, Lanke G, Langenfeld J. Bone morphogenetic protein type I receptor antagonists decrease growth and induce cell death of lung cancer cell lines. PLoS One. 2013; 8(4):e61256. Epub 2013/04/18. [PubMed: 23593444]
27. Lee YC, Cheng CJ, Bilen MA, Lu JF, Satcher RL, Yu-Lee LY, et al. BMP4 promotes prostate tumor growth in bone through osteogenesis. Cancer Res. 2011; 71(15):5194–5203. Epub 2011/06/15. [PubMed: 21670081]
28. Hao J, Ho JN, Lewis JA, Karim KA, Daniels RN, Gentry PR, et al. In vivo structure-activity relationship study of dorsomorphin analogues identifies selective VEGF and BMP inhibitors. ACS Chem Biol. 2010; 5(2):245–253. Epub 2009/12/22. [PubMed: 20020776]
29. Hill CR, Sanchez NS, Love JD, Arrieta JA, Hong CC, Brown CB, et al. BMP2 signals loss of epithelial character in epicardial cells but requires the Type III TGFbeta receptor to promote invasion. Cell Signal. 2012; 24(5):1012–1022. Epub 2012/01/13. [PubMed: 22237159]
30. Cross EE, Thomason RT, Martinez M, Hopkins CR, Hong CC, Bader DM. Application of small organic molecules reveals cooperative TGFbeta and BMP regulation of mesothelial cell behaviors. ACS Chem Biol. 2011; 6(9):952–961. Epub 2011/07/12. [PubMed: 21740033]
31. Vogt J, Traynor R, Sapkota GP. The specificities of small molecule inhibitors of the TGF-b and BMP pathways. Cell Signal. 2011; 23(11):1831–1842. Epub 2011/07/12. [PubMed: 21740966]
32. Alarmo EL, Rauta J, Kauraniemi P, Karhu R, Kuukasjarvi T, Kallioniemi A. Bone morphogenetic protein 7 is widely overexpressed in primary breast cancer. Genes Chromosomes Cancer. 2006; 45(4):411–419. Epub 2006/01/19. [PubMed: 16419056]
33. Alarmo EL, Kuukasjarvi T, Karhu R, Kallioniemi A. A comprehensive expression survey of bone morphogenetic proteins in breast cancer highlights the importance of BMP4 and BMP7. Breast Cancer Res Treat. 2007; 103(2):239–246. Epub 2006/09/28. [PubMed: 17004110]
34. Alarmo EL, Korhonen T, Kuukasjarvi T, Huhtala H, Holli K, Kallioniemi A. Bone morphogenetic protein 7 expression associates with bone metastasis in breast carcinomas. Ann Oncol. 2008; 19(2):308–314. Epub 2007/09/27. [PubMed: 17895257]
35. Alarmo EL, Huhtala H, Korhonen T, Pylkkanen L, Holli K, Kuukasjarvi T, et al. Bone morphogenetic protein 4 expression in multiple normal and tumor tissues reveals its importance beyond development. Mod Pathol. 2013; 26(1):10–21. Epub 2012/08/18. [PubMed: 22899288]
36. Comprehensive molecular portraits of human breast tumours. Nature. 2012; 490(7418):61–70. Epub 2012/09/25. [PubMed: 23000897]
37. Cerami E, Gao J, Dogrusoz U, Gross BE, Sumer SO, Aksoy BA, et al. The cBio cancer genomics portal: an open platform for exploring multidimensional cancer genomics data. Cancer discovery. 2012; 2(5):401–404. Epub 2012/05/17. [PubMed: 22588877]

38. Gao J, Aksoy BA, Dogrusoz U, Dresdner G, Gross B, Sumer SO, et al. Integrative analysis of complex cancer genomics and clinical profiles using the cBioPortal. Sci Signal. 2013; 6(269) pl1. Epub 2013/04/04.
39. ten Dijke P, Hill CS. New insights into TGF-beta-Smad signalling. Trends Biochem Sci. 2004; 29(5):265–273. Epub 2004/05/08. [PubMed: 15130563]
40. Fluck MM, Schaffhausen BS. Lessons in signaling and tumorigenesis from polyomavirus middle T antigen. Microbiology and molecular biology reviews : MMBR. 2009; 73(3):542–563. Table of Contents. Epub 2009/09/02. [PubMed: 19721090]
41. Payne SL, Hendrix MJ, Kirschmann DA. Paradoxical roles for lysyl oxidases in cancer--a prospect. J Cell Biochem. 2007; 101(6):1338–1354. Epub 2007/05/02. [PubMed: 17471532]
42. Barker HE, Cox TR, Erler JT. The rationale for targeting the LOX family in cancer. Nat Rev Cancer. 2012; 12(8):540–552. Epub 2012/07/20. [PubMed: 22810810]
43. Hollosi P, Yakushiji JK, Fong KS, Csiszar K, Fong SF. Lysyl oxidase-like 2 promotes migration in noninvasive breast cancer cells but not in normal breast epithelial cells. Int J Cancer. 2009; 125(2): 318–327. Epub 2009/03/31. [PubMed: 19330836]
44. Cox TR, Bird D, Baker AM, Barker HE, Ho MW, Lang G, et al. LOX-mediated collagen crosslinking is responsible for fibrosis-enhanced metastasis. Cancer Res. 2013; 73(6):1721–1732. Epub 2013/01/25. [PubMed: 23345161]
45. Chen JC, Chang YW, Hong CC, Yu YH, Su JL. The Role of the VEGF-C/VEGFRs Axis in Tumor Progression and Therapy. Int J Mol Sci. 2012; 14(1):88–107. Epub 2013/01/25. [PubMed: 23344023]
46. Su JL, Yen CJ, Chen PS, Chuang SE, Hong CC, Kuo IH, et al. The role of the VEGF-C/VEGFR-3 axis in cancer progression. Br J Cancer. 2007; 96(4):541–545. Epub 2006/12/14. [PubMed: 17164762]
47. Laoui D, Movahedi K, Van Overmeire E, Van den Bossche J, Schouppe E, Mommer C, et al. Tumor-associated macrophages in breast cancer: distinct subsets, distinct functions. Int J Dev Biol. 2011; 55(7–9):861–867. Epub 2011/12/14. [PubMed: 22161841]
48. He XC, Zhang J, Tong WG, Tawfik O, Ross J, Scoville DH, et al. BMP signaling inhibits intestinal stem cell self-renewal through suppression of Wnt-beta-catenin signaling. Nat Genet. 2004; 36(10):1117–1121. Epub 2004/09/21. [PubMed: 15378062]
49. Nishimori H, Ehata S, Suzuki HI, Katsuno Y, Miyazono K. Prostate cancer cells and bone stromal cells mutually interact with each other through bone morphogenetic protein-mediated signals. J Biol Chem. 2012; 287(24):20037–20046. Epub 2012/04/26. [PubMed: 22532569]
50. Katsuno Y, Hanyu A, Kanda H, Ishikawa Y, Akiyama F, Iwase T, et al. Bone morphogenetic protein signaling enhances invasion and bone metastasis of breast cancer cells through Smad pathway. Oncogene. 2008; 27(49):6322–6333. Epub 2008/07/30. [PubMed: 18663362]
51. Hao J, Ho JN, Lewis JA, Karim KA, Daniels RN, Gentry PR, et al. In vivo structure-activity relationship study of dorsomorphin analogues identifies selective VEGF and BMP inhibitors. ACS Chem Biol. 2010; 5(2):245–253. Epub 2009/12/22. [PubMed: 20020776]
52. Morrissey C, Brown LG, Pitts TE, Vessella RL, Corey E. Bone morphogenetic protein 7 is expressed in prostate cancer metastases and its effects on prostate tumor cells depend on cell phenotype and the tumor microenvironment. Neoplasia. 2010; 12(2):192–205. Epub 2010/02/04. [PubMed: 20126477]
53. Dai J, Keller J, Zhang J, Lu Y, Yao Z, Keller ET. Bone morphogenetic protein-6 promotes osteoblastic prostate cancer bone metastases through a dual mechanism. Cancer Res. 2005; 65(18): 8274–8285. Epub 2005/09/17. [PubMed: 16166304]
54. Rodriguez-Martinez A, Alarmo EL, Saarinen L, Ketolainen J, Nousiainen K, Hautaniemi S, et al. Analysis of BMP4 and BMP7 signaling in breast cancer cells unveils time-dependent transcription patterns and highlights a common synexpression group of genes. BMC Med Genomics. 2011; 4:80. Epub 2011/11/29. [PubMed: 22118688]
55. Kwon SJ, Lee GT, Lee JH, Kim WJ, Kim IY. Bone morphogenetic protein-6 induces the expression of inducible nitric oxide synthase in macrophages. Immunology. 2009; 128(1 Suppl):e758–e765. Epub 2009/09/25. [PubMed: 19740337]

56. Pickup MW, Laklai H, Acerbi I, Owens P, Gorska AE, Chytil A, et al. Stromally Derived Lysyl Oxidase Promotes Metastasis of Transforming Growth Factor-beta Deficient Mouse Mammary Carcinoma. Cancer Res. 2013 Epub 2013/07/17.

57. Owens P, Engelking E, Han G, Haeger SM, Wang XJ. Epidermal Smad4 deletion results in aberrant wound healing. Am J Pathol. 2010; 176(1):122–133. Epub 2009/12/05. [PubMed: 19959815]

58. Novitskiy SV, Pickup MW, Chytil A, Polosukhina D, Owens P, Moses HL. Deletion of TGF-beta signaling in myeloid cells enhances their anti-tumorigenic properties. J Leukoc Biol. 2012; 92(3): 641–651. Epub 2012/06/12. [PubMed: 22685318]

59. Novitskiy SV, Pickup MW, Gorska AE, Owens P, Chytil A, Aakre M, et al. TGF-beta receptor II loss promotes mammary carcinoma progression by Th17 dependent mechanisms. Cancer Discov. 2011; 1(5):430–441. Epub 2012/03/13. [PubMed: 22408746]

60. Gyorffy B, Lanczky A, Eklund AC, Denkert C, Budczies J, Li Q, et al. An online survival analysis tool to rapidly assess the effect of 22,277 genes on breast cancer prognosis using microarray data of 1,809 patients. Breast Cancer Res Treat. 2010; 123(3):725–731. Epub 2009/12/19. [PubMed: 20020197]

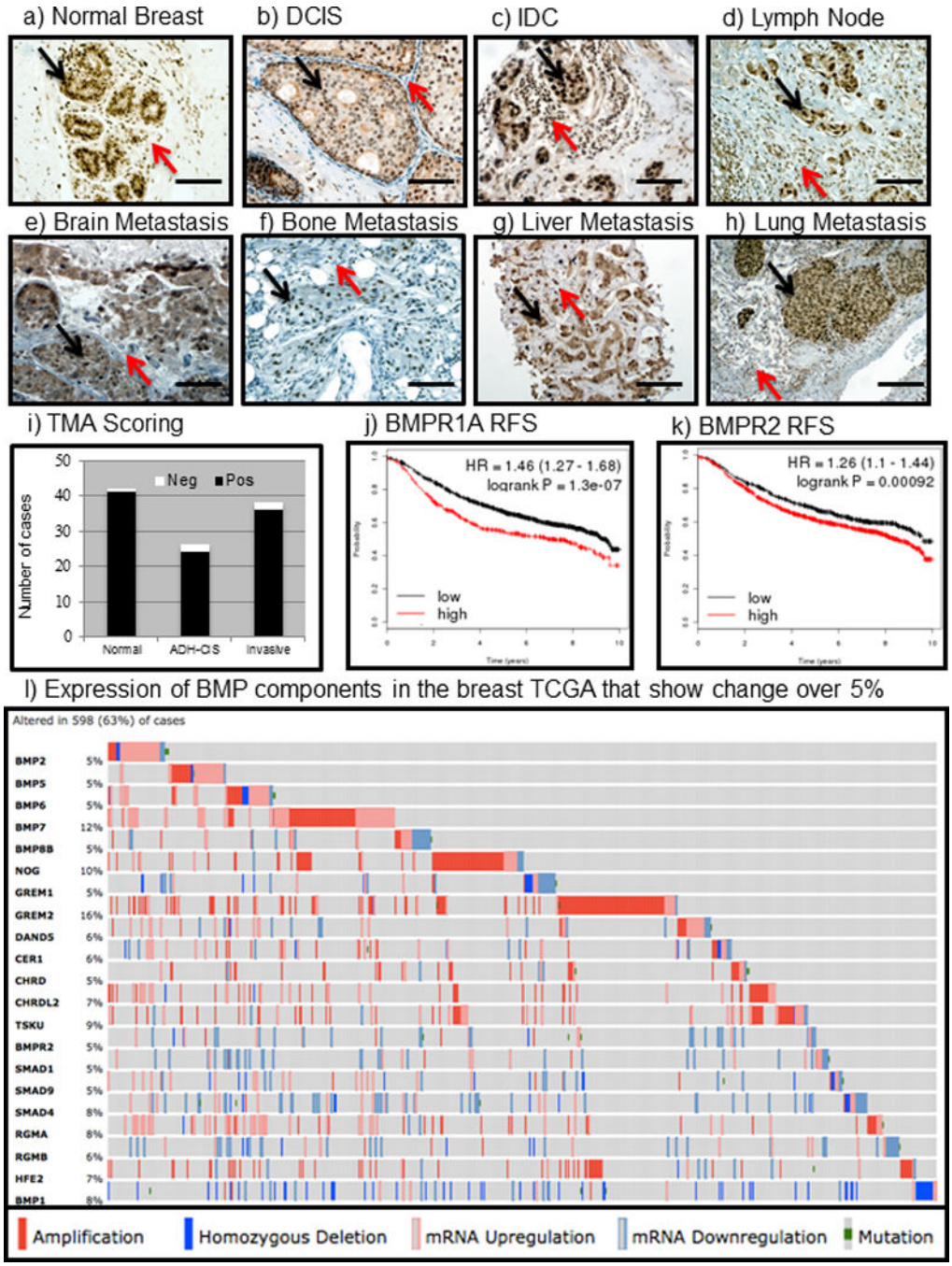

Figure 1. Bone Morphogenetic Protein signaling is active in human breast cancers and is rarely absent

a) IHC for pSmad1/5/9 demonstrates that the BMP pathway is active in normal breast both in the epithelium (black arrow) and in the surrounding stroma (red arrow). b) In pre-cancerous DCIS lesions, heterogeneous staining showing BMP activation in both the epithelium (black arrow) as well as the surrounding stroma (red arrow). c) BMP signaling is quite strong and active in IDC not only in the primary tumor (black arrow) but also in the stromal infiltrates surrounding the tumor (red arrow). d–f) In metastases to the lymph node (d), brain (e), bone (f), liver (g), and lung (h) tumors exhibited strong staining for active

BMP signaling in tumor cells (black arrows) as well as the tumor microenvironment (red arrows). i) IHC for pSmad1/5/9 was performed on two tissue microarrays purchased from US bio max catalog #'s 480 and 722 which contained normal breast, pre-cancerous hyperplasia's and invasive cancers. Scoring revealed that normal breast were 41/42 positive, ADH-CIS were 24/26 positive and Invasive cancers were 36/38 positive for pSmad1/5/9. j) BMP receptor IA (BMPR1A) was queried for correlation to overall survival of breast cancer patients using kmplot.com and found that high expression (red) correlated with poor survival (logrank P =1.3e-^{07}). k) The type II BMP receptor BMPR2 high expression correlated with poor survival using kmplot.com (logrank P =0.00092). l) Using the cBio portal (cbioportal.org) to investigate BMP signaling components in the TCGA we found that in the provisional breast database consisting of 950 total samples 21 BMP related genes altered in greater than 5% of all patients. Solid dark red boxes indicate copy number amplification, light pink indicates mRNA upregulation, dark blue indicates homozygous deletion, light blue indicates mRNA downregulation and green boxes indicate mutations. Microscope scale bars = 100μM. Abbreviations: ADH, Atypical Ductal Hyperplasia. DCIS, Ductal Carcinoma In-Situ. IDC, Invasive Ductal Carcinoma. TMA, Tissue Micro-Array. RFS, Relapse Free Survival. TCGA, The Cancer Genome Atlas. IHC, Immunohistochemistry.

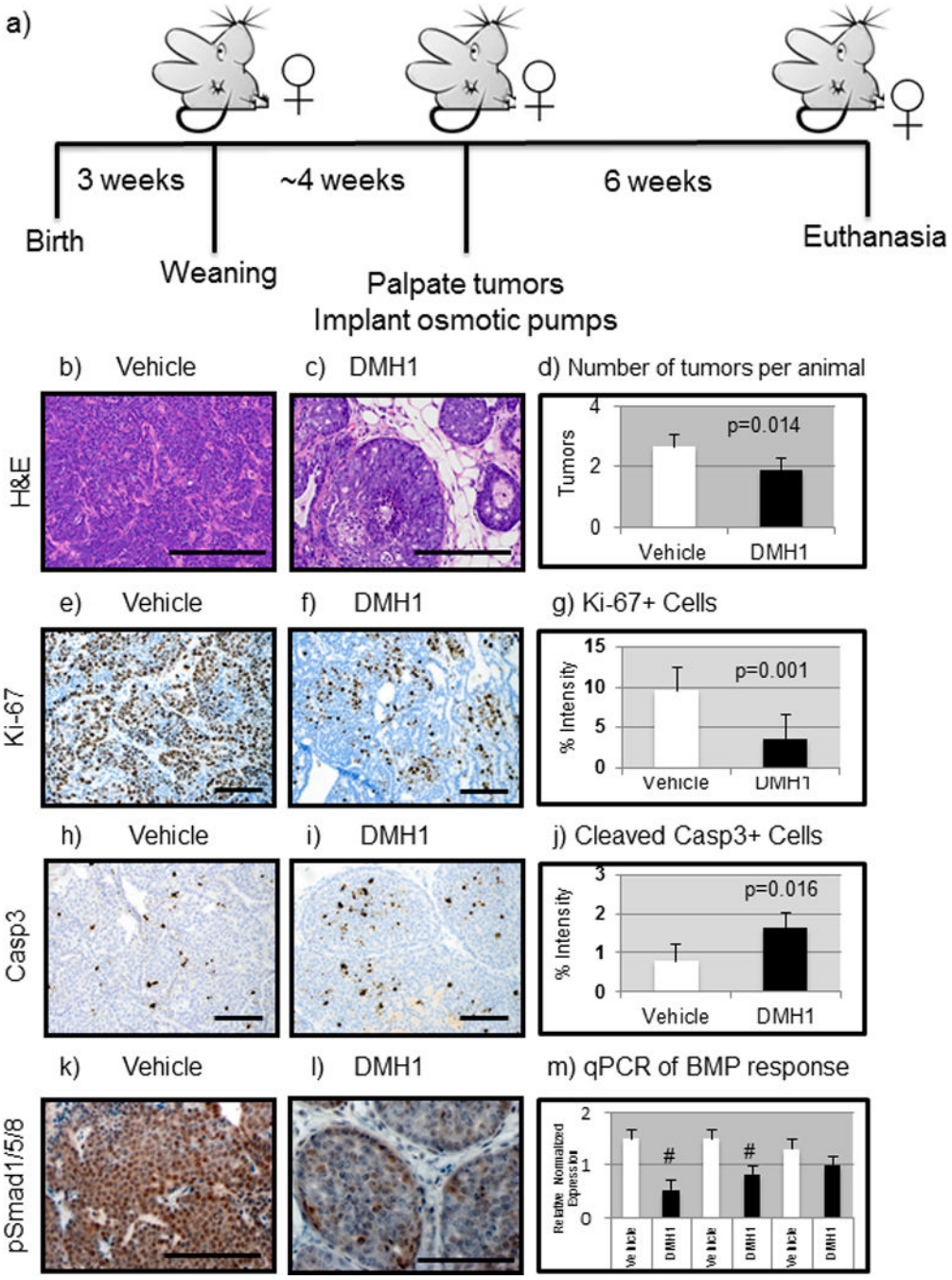

Figure 2. Mice treated with DMH1 reduce primary mammary tumor growth

a) FVBn mice expressing the MMTV.PyVmT constitutively expressed oncogene were implanted with slow release (6 weeks) osmotic pumps after first palpation of tumors (~7weeks). b) Vehicle (DMSO only, n=12) treated tumors were stained with H&E which indicated advanced adenocarcinoma morphology. c) DMH1 treated animals (n=12) revealed a much less advanced adenocarcinoma appearance. d) The number of tumors per animal greater than .5cm in diameter were counted at sacrifice and revealed a statistically significant (P=0.014) reduction with DMH1 treatment (1.92) compared to vehicle treated

controls (2.66). e) IHC for Ki-67 to indicate actively proliferating cells revealed strongly proliferative cells in vehicle treated animals. f) DMH1 treated tumors revealed less actively stained Ki-67+ cells. g) IHC for the proliferation marker Ki-67 showed significant (P=0.001) reduction in proliferating tumor cells (vehicle=9.52, DMH1=3.61). h) IHC for activation of apoptosis via cleavage of caspase 3 revealed little apoptosis in vehicle treated primary tumors. i) DMH1 treated tumors displayed significantly higher levels of activated caspase 3 by IHC. j) Quantitation of IHC for apoptosis maker cleaved-caspase3 showed significant (P=0.016) increase in apoptotic tumor cells (vehicle=.79, DMH1=1.62). k) IHC for active BMP signaling with pSmad1/5/8 demonstrated that primary tumors are strongly positive for BMP signaling. l) DMH1 treated tumors had reduced staining for pSmad1/5/8 indicating reduced yet not absent BMP signaling. m) EpCAM+ tumor cells isolated by FACS had RNA isolated and SYBR qPCR was performed for BMP transcriptional targets, which demonstrated a significant reduction in *Id1* and *Smad6*. Normalized expression for qPCR was performed in comparison to GAPDH expression. Quantification of IHC was performed using NIH ImageJ software to detect pixels positive for stain in a 20X field of view. A minimum of four tumors with at least five representative images were used in analysis. # Indicate statistical significance (P=<0.05) by performing a student's T-test. Error bars indicate SEM.

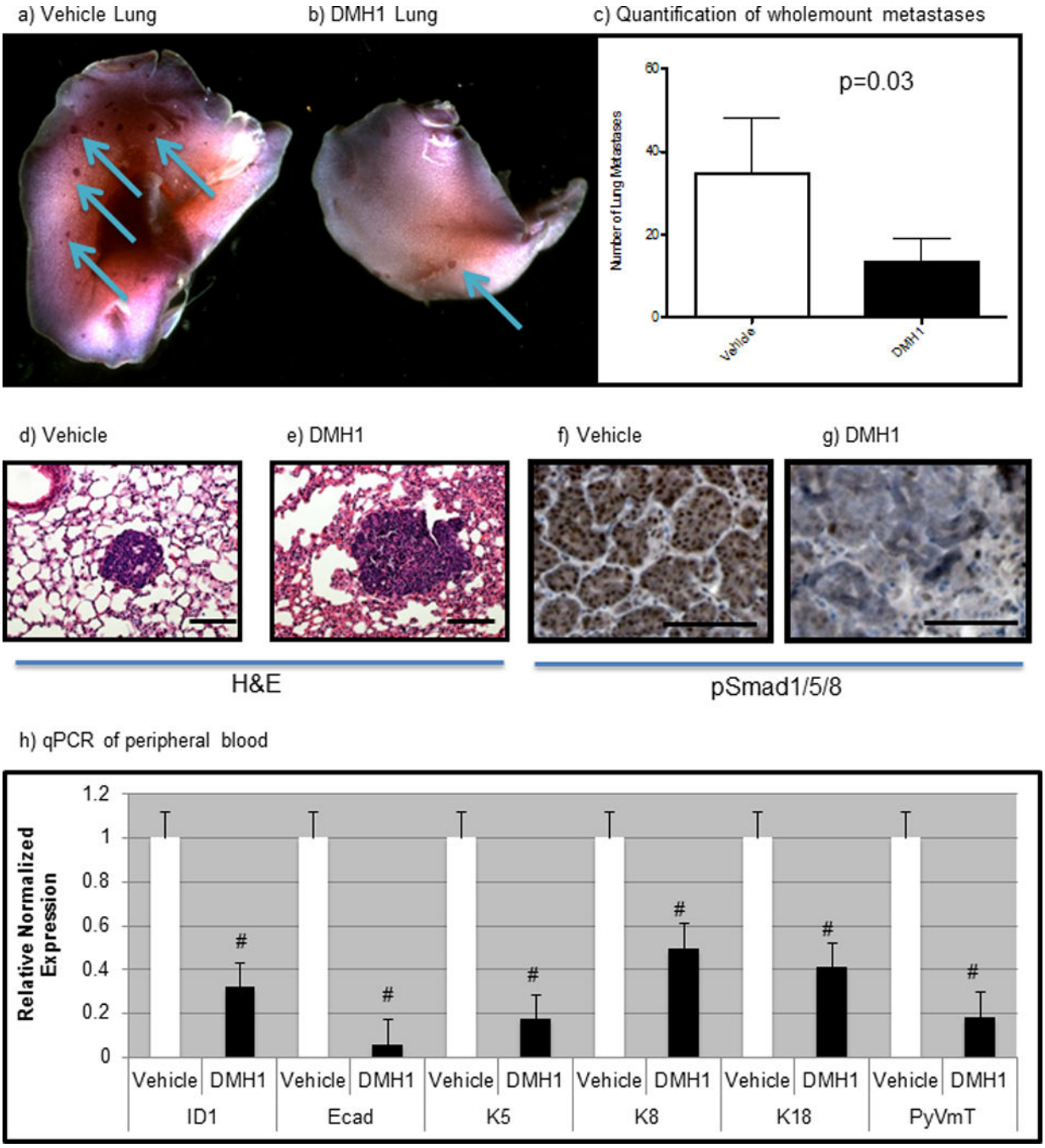

Figure 3. The BMP receptor kinase antagonist DMH1 reduces metastases in the MMTV-PyVmT transgenic mouse model of breast cancer

a) Control mice treated with vehicle (DMSO) showed typical lung metastatic burden after 6 weeks from the palpation of the primary tumor. b) Animals treated with DMH1 for 6 weeks following initial tumor palpation had far fewer lung metastases. c) Metastases were counted in lung whole mounts from a total number of 12 control and 12 DMH1 treated mice and demonstrated a statistically significant reduction in lung metastases (P=0.03). d–e) H&E staining of lung metastases confirmed that whole mount stained lungs contained metastatic tumor cells. f) IHC for pSmad1/5/8 demonstrated that spontaneous lung metastases

contained strongly active BMP signaling. g) DMH1 treated animals lungs indicated reduced activity in BMP signaling by pSmad1/5/8. h) Peripheral blood was collected by cardiac puncture at the time of sacrifice and RNA was isolated. SYBR qPCR was performed to detect circulating tumor cells where markers for the tumors all showed reduction in DMH1 treated animals. *Id1* transcription, which is the canonical indicator of BMP transcription, was significantly reduced in the peripheral blood of DMH1 treated animals. Microscope scale bars = 100μM. # Indicate statistically significant by students T-test. Error bars for qPCR and metastases quantification indicate SEM.

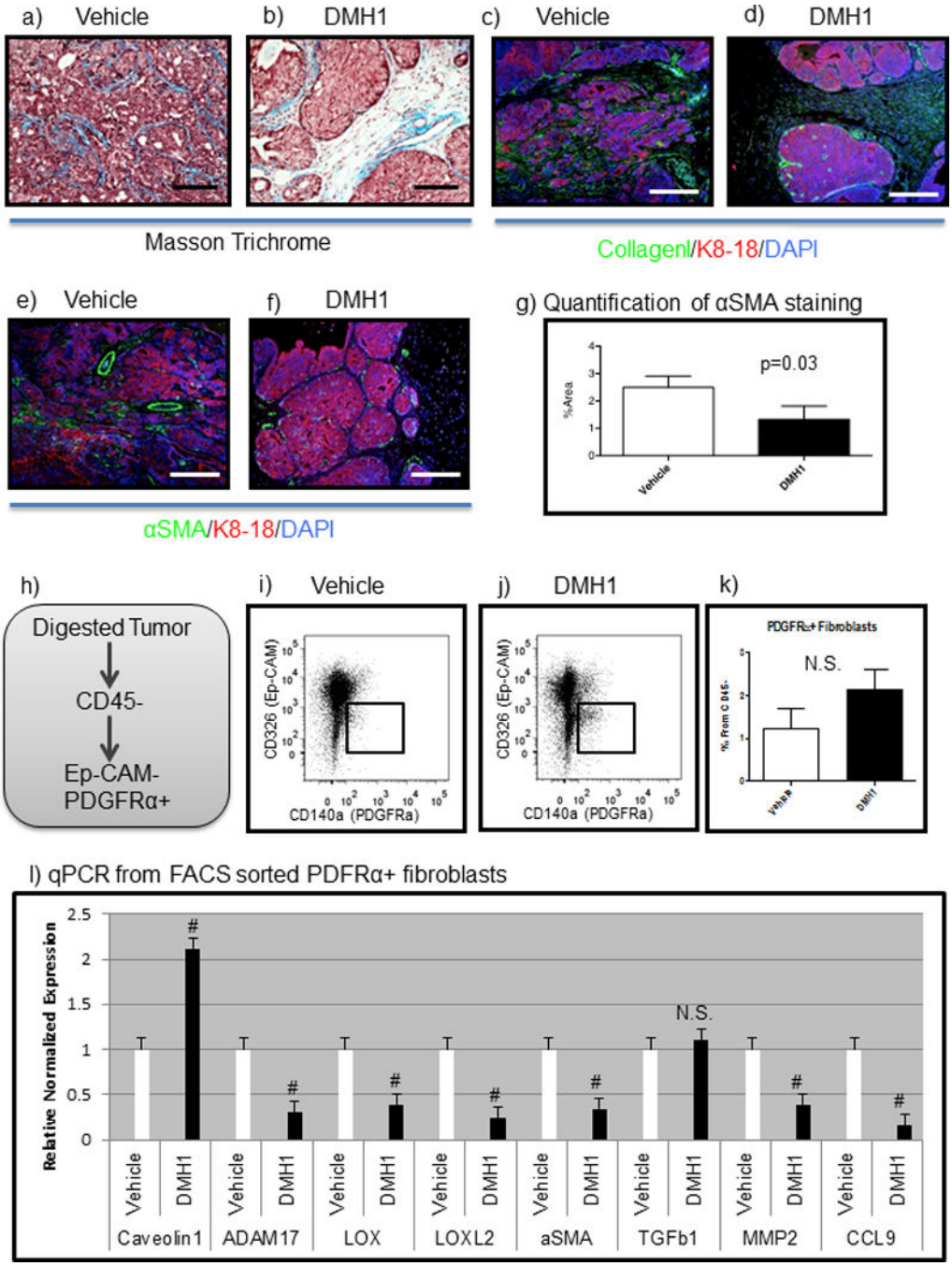

Figure 4. DMH1 treatment alters tumor associated fibroblasts

a) Masson trichrome staining reveals collagen (aniline blue staining) distribution intra-tumorally in vehicle treated tumors. b) DMH1 treated tumors revealed less collagen staining in the stroma. c–d) IF staining for Collagen I (green), tumor epithelium is highlighted by K8-18 (red) staining and total nuclei are stained with DAPI (blue). e–f) IF staining for the myofibroblast marker for αSMA (green) g) Quantification of αSMA staining in primary tumors revealed statistically significant (P=0.03) changes in %Area of αSMA staining in primary tumors. h) FACS isolation of fibroblasts was performed by digesting primary

tumors and negatively selecting for CD45+ cells, dead cells and EpCAM+ cells. Positive selection of PDGFRα+ cells were sorted and RNA was isolated followed with SYBR qPCR. i–k) Flow cytometry analysis of tumor associated fibroblasts revealed a trending increase in fibroblasts per tumor in DMH1 treated tumors than controls. l) SYBR qPCR of sorted tumor associated fibroblasts revealed unique transcriptional differences in fibroblasts treated with DMH1 compared with vehicle controls. Microscope scale bars = 100μM. # Indicate statistically significant by students T-test. Error bars for Picrosirius quantification indicate SD. Error bars for qPCR and flow cytometry indicate SEM. Abbreviations αSMA alpha-smooth muscle actin. NS=Not Significant.

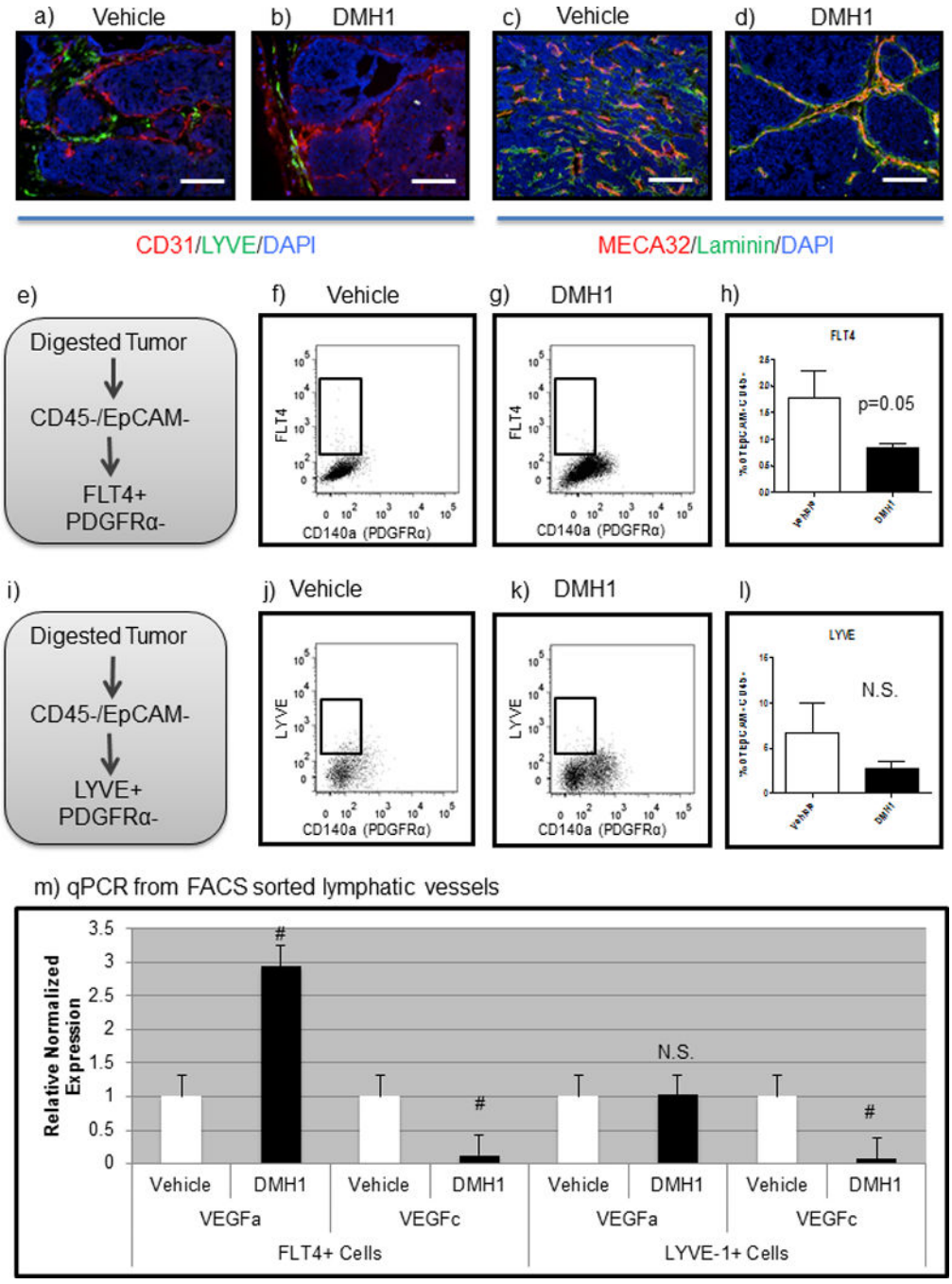

Figure 5. DMH1 treatment inhibits lymphangiogenesis

a) IF staining for blood vessels by CD31 (red) and lymphatic vessels by LYVE (green) reveals that vehicle treated animals have vessels infiltrated within the tumor mass. b) DMH1 treated tumors demonstrate blood vessels throughout the tumor yet lymphatics are restricted peri-tumorally. c–d) IF staining for total vessels by MECA32 (red) intra-tumorally highlight the phenotypic architecture of vessels adjacent to the basement membrane shown by Laminin (green) staining. e) Flow cytometry of primary tumors isolated cells by negative selection of dead cells, CD45+ and EpCAM+ cells. FLT4+ cells that were PDGFRα

negative were analyzed in f–g. h) Quantitation of FLT4+ lymphatic cells demonstrated a significant reduction in lymphatic specific vessels with DMH1 treatment compared to vehicle control treated tumors/mice. i) Flow cytometry for the lymphatic maker LYVE with negative selection of dead cells, CD45+, EpCAM+ and PDGFRα+ were excluded and analyzed in j–k. l) Quantitation of LYVE+ cells revealed a trending decrease in DMH1 treatment compared to vehicle controls. m) FACS sorted FLT4+ and LYVE+ cells from both vehicle and DMH1 primary tumors both demonstrated a significant reduction in lymphatic specific reduction of *VEGFc* and not *VEGFa* transcription. Microscope scale bars = 100μM. # Indicate statistically significant by students T-test. Error bars for qPCR and flow cytometry indicate SEM.

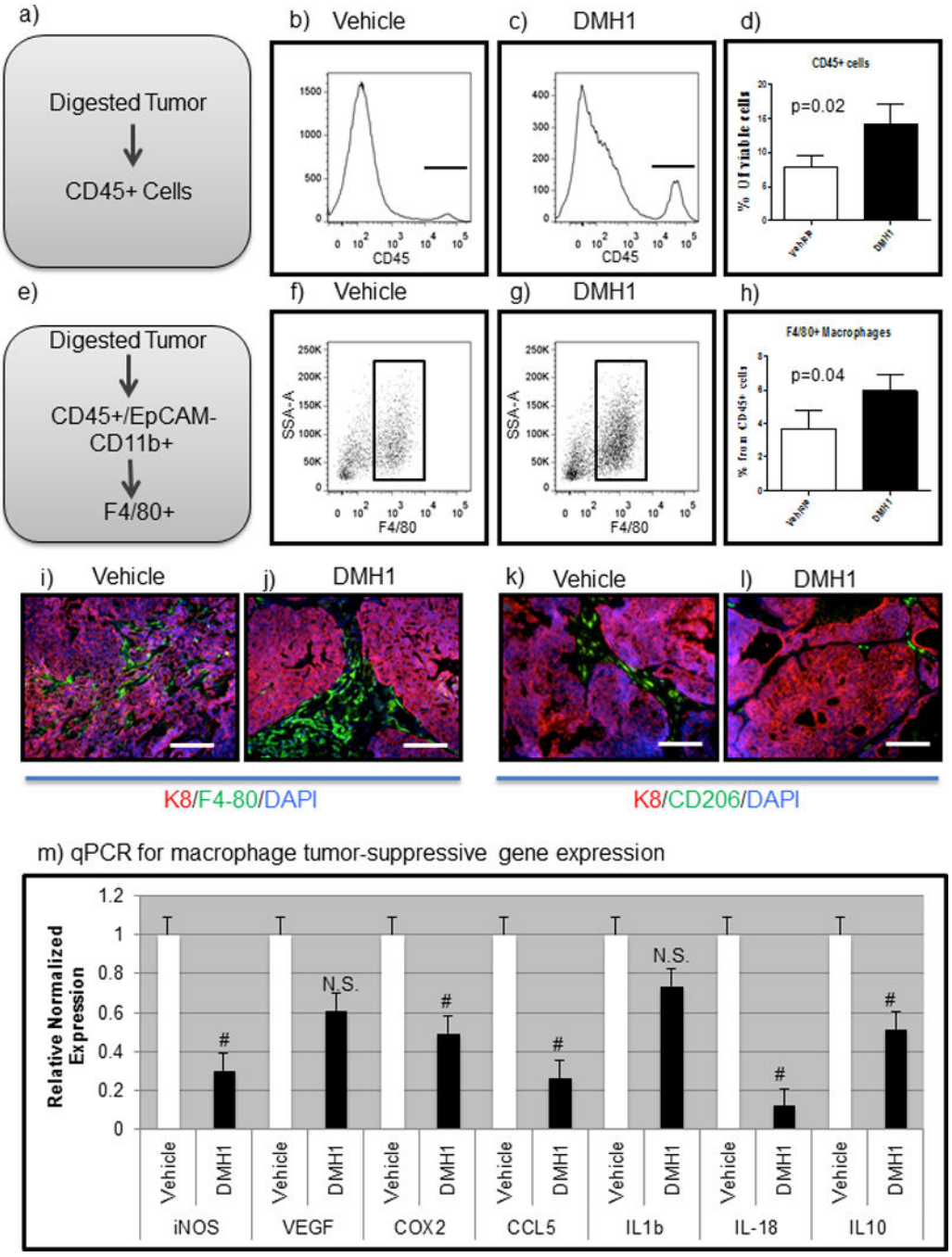

Figure 6. DMH1 inhibition for BMP signaling alters the immune response in primary tumors

a-c) Primary tumors were digested and stained for viable CD45+ cells. d) DMH1 treated tumors demonstrated significantly increased immune cells than vehicle controls. e–g) Macrophage cells were significantly increased in DMH1 tumors as compared to vehicle controls. i–j) IF Staining for F4/80 macrophages (green) were identified within the tumor center as compared to DMH1 treated tumors which were located mostly peri-turmorally (j). k–l) Tumor promoting macrophages (CD206-green) were more abundant in vehicle treated tumors than DMH1 treated. m) FACS sorting for F4/80+ macrophages revealed distinct

polarization in DMH1 tumors to be less tumor promoting than vehicle isolated macrophages with significant reductions in inflammatory cytokines. Microscope scale bars = 100μM. # Indicate statistically significant by students T-test. Error bars for qPCR and flow cytometry indicate SEM.

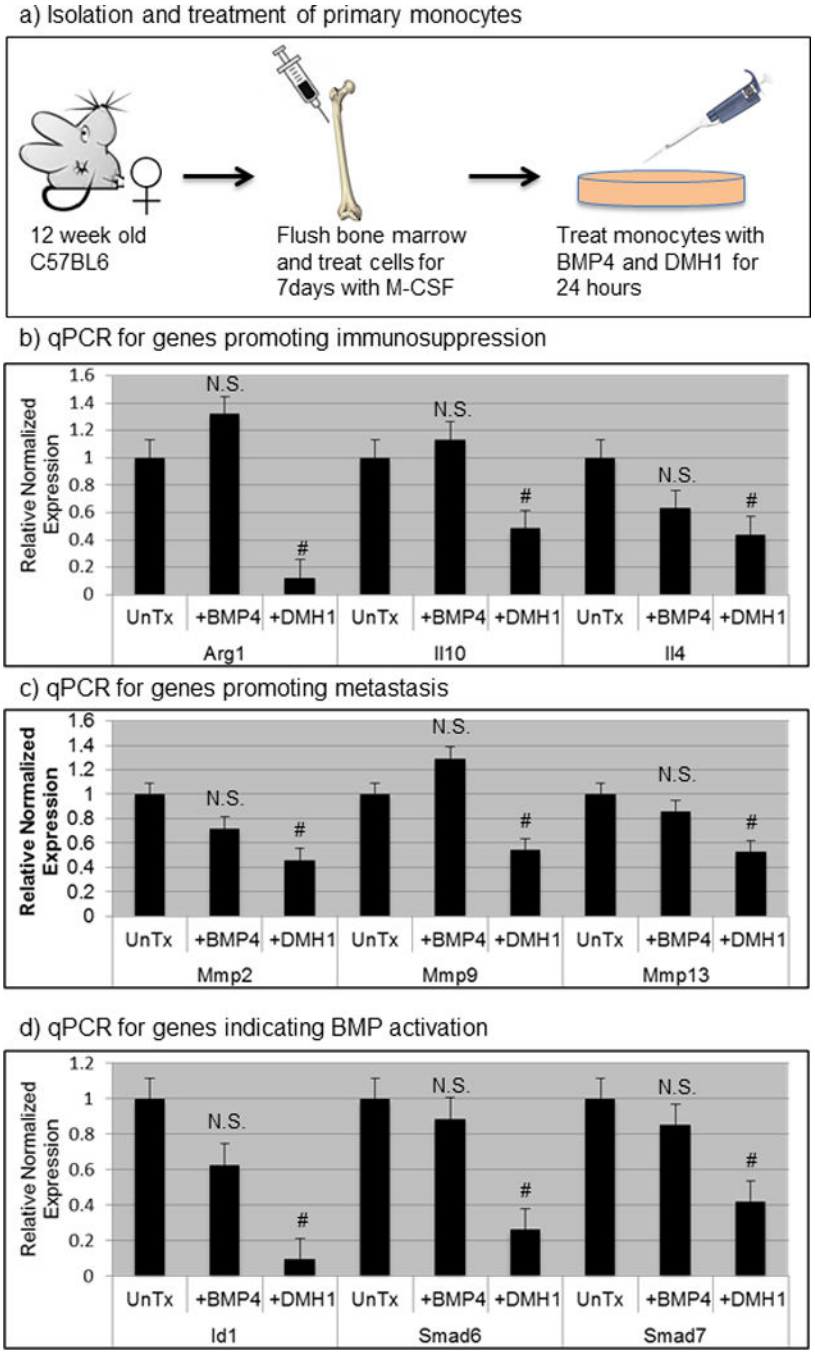

Figure 7. DMH1 inhibition of primary monocytes results tumor suppressive gene expression

a) Cartoon schematic demonstrating how primary monocytes were isolated from bone marrow. Bone marrow flush was performed in triplicate mice and converted to monocytes with the addition of M-CSF for 7 days and then cells were untreated(UnTx), treated with 100ng/ml of BMP4, or treated with both 100ng/ml of BMP4 and 20uM of DMH1 for 24 hours. b–d) qPCR genes involved in immune suppression, metastasis and the canonical BMP pathway activation were normalized to the housekeeping gene beta-actin and further normalized to relative to untreated monocyte mRNA expression. # indicates statistically

significant (p=<.05) by students T-test. Error bars indicate SEM. N.S. Not Significant (p=>.05)